edX Silicon Photonics Design, Fabrication and Data Analysis Final Report

G. Simpson, edX username: Garen123

***Abstract*—This report discusses the rapid design, fabrication, and characterization of Mach-Zehnder Interferometers (MZIs) on a Silicon-On-Insulator (SOI) platform. Using standard design techniques and polynomial fitting, optical parameters such as effective index, group index, and optical dispersion are extracted from component-level simulations and experimental data. The devices were fabricated using the NanoSOI multi-project wafer process with electron beam lithography and plasma-enhanced chemical vapor deposition (PECVD) cladding, the devices were tested using a fully automated fiber-coupled optical setup. Background-subtracted spectral responses for determining the group indices and free spectral ranges (FSRs) for two MZIs with different path length differences were analyzed. Corner analysis was performed to assess fabrication induced variability on the devices, confirming that the experimentally determined group indices fall within the predicted ranges based on manufacturing tolerances. A Monte Carlo simulation quantifying the expected FSR variation was conducted, validating the experimental findings. The results illustrate that rapid prototyping combined with effective modeling techniques can produce reliable integrated photonic circuits suitable for signal processing and sensing applications. This report highlights the practical use of silicon photonics design workflows and provides a scalable methodology for assessing performance under realistic fabrication variations.**

I. INTRODUCTION

Silicon photonics is the combination of developments in microelectronics and photonics that allows for using light to make technological advancements in areas relating to communications, information processing, and sensing applications, all in a compact microchip. Silicon possesses unique qualities such as transparency around wavelengths 1.3 – 1.8um, especially relevant for tele-communications networks. It is properties such as this, along with an established complementary metal oxide semiconductor (CMOS) industry that has allowed it to become especially prevalent in recent advances in data transfer for artificial intelligence applications [1].

The importance of silicon photonics is further emphasized when looking at the energy efficiency of using light to move information rather than electrical circuits. As our understanding of how to move vast amounts of information in optical fibers is understood, it can be applied to silicon photonics to enable to efficient transfer of information in datacenters as witnessed by companies like Nvidia. Behind all of this is an industry built on rapid design and fabrication of integrated photonic circuits.

To implement rapid design and fabrication of high-performance silicon photonic components. Resources such as Process Design Kits, multi-project wafer runs, and automatic testing are critical. This edX course on Silicon Photonics Design, Fabrication and Data Analysis demonstrates this process in the production of integrated photonic circuits with Mach Zehnder Interferometers as an example. A widely used component in optics and photonics for demonstrating the principle of interferometry, made from assembling grating couplers, splitters and optical waveguides.

This paper will demonstrate the principles behind the rapid design and fabrication of Mach Zehnder Interferometers on a silicon on insulator platform (SOI), made from grating couplers, y-splitters and wire optical waveguides. The results of the Mach Zehnder components will allow for interpreting determining parameters such as free spectral range, refractive index, group index and dispersion of the device.

II. THEORY

To properly understand the properties of an MZI, the effective index of the waveguides, splitting ratio of the y-branches and coupling loss of the grating couplers must be understood. The effective index is a measure of the average refractive index light experiences in a guided optical mode in a waveguide. Guided modes can have effective index values that range from higher than the index of the cladding material (n_1) to lower than the refractive index of the core material (n_2). Depending on this effective index, the propagation of the light can vary from well confined within the guiding core material, or leak out into the cladding, this is what can affect the dispersion of the optical mode. Some unique waveguide geometries have been designed to take advantage of modes that are confined less to the core material such as slot waveguides and subwavelength grating waveguides, however in this report we will be looking at wire waveguides [2] [3].

Understanding the effective index allows us to calculate other parameters such as the group index and dispersion, a polynomial expansion of the effective index given enough data within a sufficient wavelength range to draw a polynomial curve fit.

$$n_{eff}(\lambda) = A_1 + A_2(\lambda - \lambda_0) + A_3(\lambda - \lambda_0)^2$$

Where A_1 is the refractive index, A_2 is used to find the group index and A_3 is used to find the dispersion using the equations below The effective index data can be used to find polynomial coefficients which can describe the group index as

well as dispersion ($ps\ /\ nm\ Km$). For a nominal waveguide design of 500nm x 220nm which achieves single mode transverse electric (TE) propagation for the SOI platform. A_1 is the refractive index, A_2 is used to find the group index and A_3 is used to find the dispersion using the equations below.

$$A_1 = 2.4446$$

$$A_2 = -1.12647$$

$$A_3 = -0.03321$$

$$n_{eff}(\lambda) = 2.4446 - 1.12647(\lambda - \lambda_0) - 0.0332114\lambda(-\lambda_0)^2$$

Refractive index = 2.4446

$$Ng\ = A_1 - A_2 * (\lambda_0) = 4.192$$

$$D = -\frac{\lambda}{c} 2A_3 = 343.4\ \frac{ps}{nm\ Km}$$

A Mach Zehnder interferometer is a device that uses light travelling in two different paths to introduce a phase difference between them before being recombined. In a simple MZI, the light intensity is split equally into two different paths using a component such as a y-splitter, directional coupler or multimode interferometer (MMI). The two paths then cause a phase difference through either a path length difference in the arms, or a change in the refractive index caused by thermo or electro-optic manipulation [4]. The beams are then combined again using a y-splitter or directional coupler and the output intensity will vary as a function of the phase shift between the paths, yielding a free spectral range (FSR) which can be used to determine the group index. This is described by the transfer function equations for the MZI below.

$$\frac{I_o}{I_i} = \frac{1}{2}[1 + \cos(\beta_1 L_1 - \beta_2 L_2)]$$

$$\beta(\lambda) = \frac{2\pi\, n_{eff}(\lambda)}{\lambda} + i\frac{\alpha}{2}$$

$$T_{MZI}(\lambda) = |1 + e^{-i\beta(\lambda)\Delta L}|^2$$

$$FSR = \frac{\lambda^2}{\Delta L n_g}$$

Where β is the propagation constant in the respectrive arms, ΔL is the path length difference, n_g is the group index, and α is the propagation loss. In the MZI 0% transmission occurs for phase shifts of π. we can find the group index of a device such as Mach Zehnder interferometer from the FSR described above where the FSR is the peak-to-peak distance in wavelength Δλ between the minima or maxima. Propagation losses can be included in the α term for the propagation function β(λ).

The use of the effective index allows for a quick and easy prediction of the performance of the MZI when considering FSR and group index. For determining the effect of losses, both coupling and propagation in the performance. Data from component level simulations is valuable.
To understand how the change in the path length difference in the arms of the MZI affects the free spectral range, the table below shows the expected FSR values for a range of ΔL from 50 -200 μm as well as the image of the MZI transfer function for 50μm and 100μm. As the ΔL increases the FSR becomes smaller.

Table I: Free Spectral Range for increasing path lengths at a wavelength operation of 1550 nm and group index of 4.2.

Path length Difference (ΔL) [μm]	Free Spectral Range [nm]
50	11.44
100	5.72
150	3.81
200	2.86

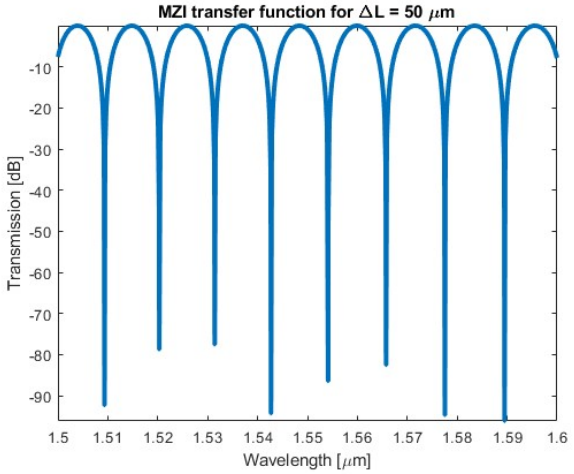

Figure 1: MZI transfer function for a path length difference of 50um.

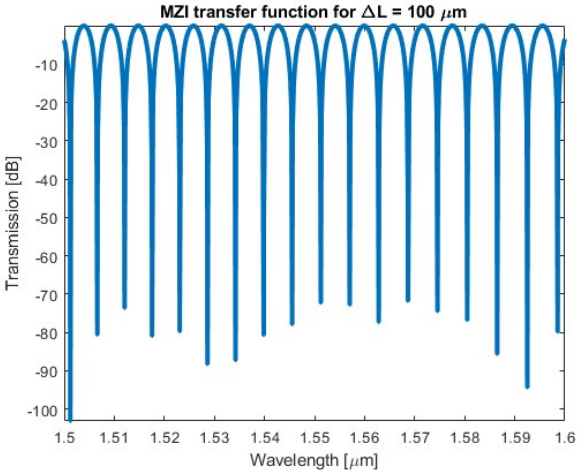

Figure 2: MZI transfer function for a path length difference of 100um

III. Modelling and simulation

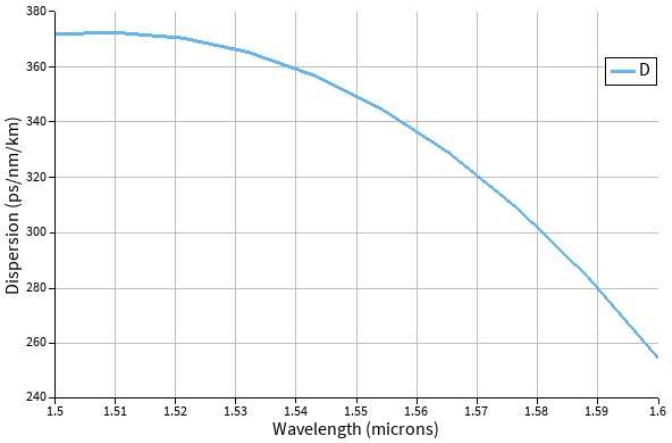

Figure 3 dispersion vs wavelength for a 500 nm width x 220 nm height SOI waveguide

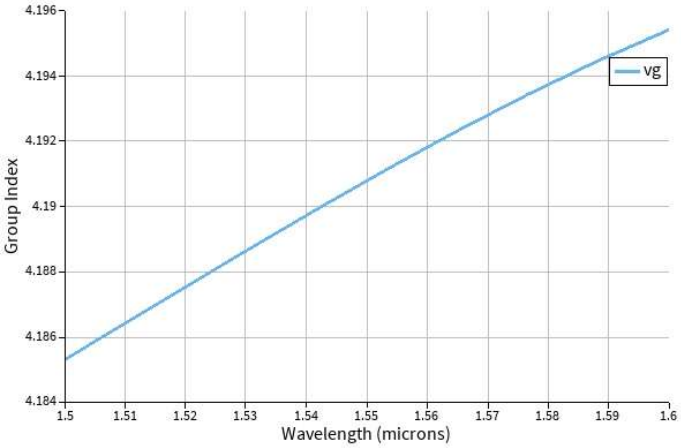

Figure 4: group index vs wavelength for a 500 nm x 220 nm SOI waveguide

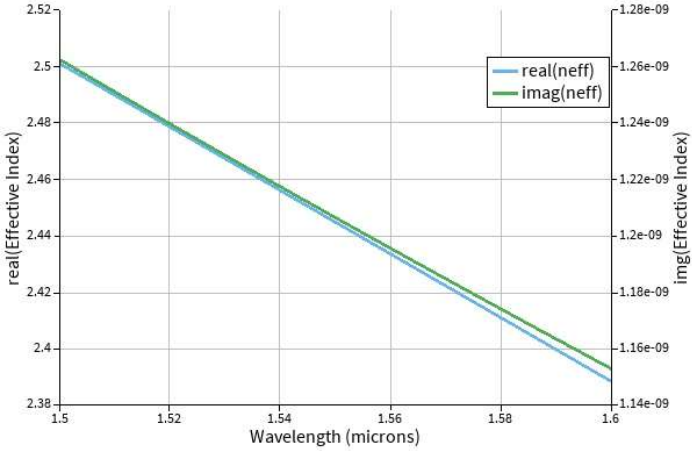

Figure 5: Neff vs wavelength for a 500 nm x 220 nm SOI waveguide

Waveguide and circuit geometry

In the circuit, the highlighted MZI's are discussed in this report with respective path length differences of approximately 56.7nm and 971 nm. The other MZI circuits incorporate subwavelength structures that are not discussed in this course but can be used in further reports on periodic waveguiding structures.

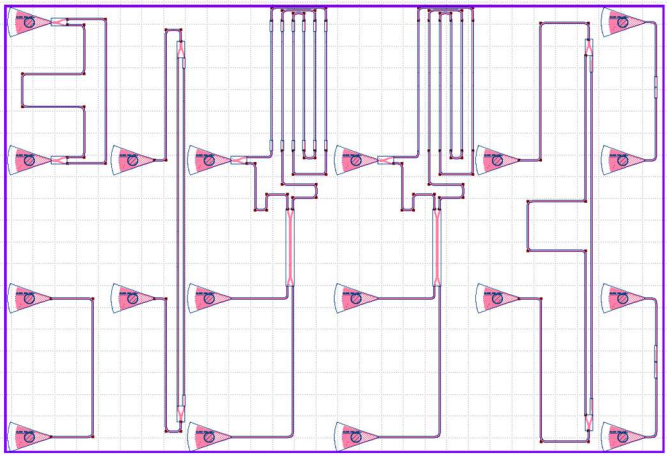

Figure 6: GDS layout for SOI fabrication. MZI1 top left. MZI4 fourth from the left.

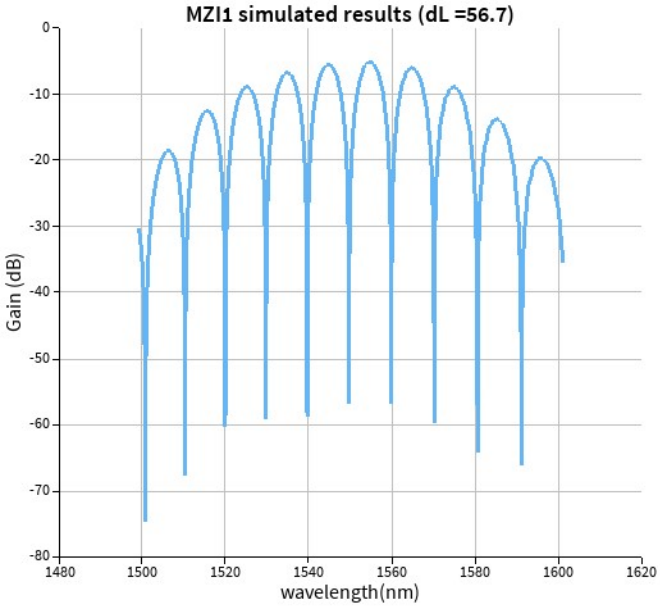

Figure 7: MZI1 simulated results for a path length difference of approximately 56.7um

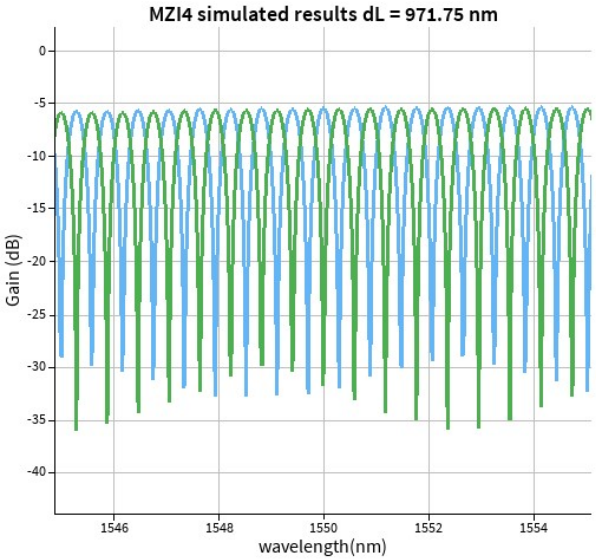

Figure 8: MZI4 simulated results for a path length difference of approximately 971 um.

IV. Corner analysis

To determine the variation of the parameters of the circuit, such as the group index, and free spectral range, the standard deviations for wafer variability and feature size ar given by the manufacturing process and used in determining the minimum and maximum group index variations as a result. The wafers used for the silicon on insulator fabrication process have an average thickness of 219 nm and a 6 σ distribution of 23.4nm giving a thickness of 219 +/- 11.9nm for virtually all devices. Using one standard deviation we arrive at an average thickness of 219nm +/- 3.9nm. This gives us a minimum of approximately 215nm and maximum thickness of 223nm. For the feature size variation, we will assume a variation of 40nm, and the waveguide width will vary between 470nm to 510nm.

For minimum waveguide features of 215nm thickness and 470nm width and maximum feature sizes of 223nm and 510nm we will see the main parameter of investigation, the group index, change from a minimum value to a maximum value. This will give us a way to judge the circuit performance because of fabrication variability. If the group index values fall within the minimum and maximum, we can assume a good fabrication process.

Table 2: Corner Analysis of SOI waveguide

Group index values for wg variation	wg width min (470nm)	wg width max (510nm)
wg thickness min (215 nm)	4.240	4.170
wg thickness max (223 nm)	4.249	4.178

Where the green and red values indicate the highest and lowest values for the group index respectively. This gives us a $\Delta n_g = 0.079$

We can use this variability of the group index of about 0.08 in a monte Carlo simulation of the FSR variability with a range of 500 samples to determine the impact on the FSR of MZI1 using a standard deviation in the path length difference of 10nm we get the plot below with a mean FSR of 10.40nm and standard deviation of 1.90 nm, assuming a nominal value of 56.7nm for the path length difference in MZI1.

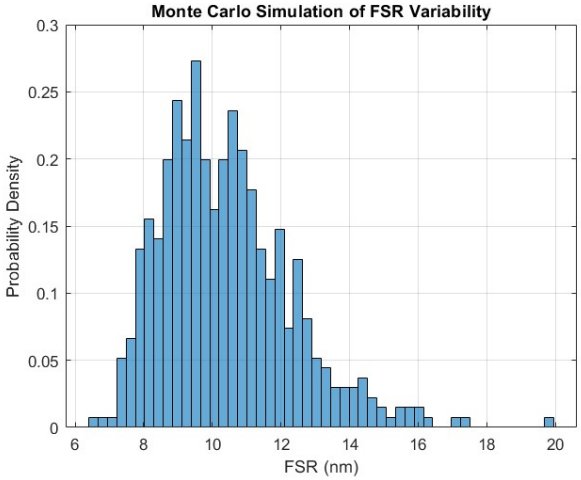

Figure 9: Monte Carlo simulation of FSR variability

V. Fabrication

The photonic devices were fabricated using the NanoSOI MPW fabrication process by Applied Nanotools Inc. (http://www.appliednt.com/nanosoi; Edmonton, Canada) which is based on direct-write 100 keV electron beam lithography technology. Silicon-on-insulator wafers of 200 mm diameter, 220 nm device thickness and 2 µm buffer oxide thickness are used as the base material for the fabrication. The wafer was pre-diced into square substrates with dimensions of 25x25 mm, and lines were scribed into the substrate backsides to facilitate easy separation into smaller chips once fabrication was complete. After an initial wafer clean using piranha solution (3:1 H2SO4:H2O2) for 15 minutes and water/IPA rinse, hydrogen silsesquioxane (HSQ) resist was spin-coated onto the substrate and heated to evaporate the solvent. The photonic devices were patterned using a Raith EBPG 5000+ electron beam instrument using a raster step size of 5 nm. The exposure dosage of the design was corrected for proximity effects that result from the backscatter of electrons from exposure of nearby features. Shape writing order was optimized for efficient patterning and minimal beam drift. After the e-beam exposure and subsequent development with a tetramethylammonium sulfate (TMAH) solution, the devices were inspected optically for residues and/or defects. The chips were then mounted on a 4” handle wafer and underwent an anisotropic ICP-RIE etch process using chlorine after qualification of the etch rate. The resist was removed from the surface of the devices using a 10:1 buffer oxide wet etch, and the devices were inspected using a scanning electron microscope (SEM) to verify patterning and etch quality. A 2.2 µm oxide cladding was deposited using a plasma-enhanced chemical vapour deposition (PECVD) process based on tetraethyl orthosilicate (TEOS) at 300ºC. Reflectometry measurements were performed throughout the process to

verify the device layer, buffer oxide and cladding thicknesses before delivery.

VI. Experimental Data collection

To characterize the devices, a custom-built automated test setup [5, 9] with automated control software written in Python was used [6]. An Agilent 81600B tunable laser was used as the input source and Agilent 81635A optical power sensors as the output detectors. The wavelength was swept from 1500 to 1600 nm in 10 pm steps. A polarization maintaining (PM) fibre was used to maintain the polarization state of the light, to couple the TE polarization into the grating couplers [7]. A 90º rotation was used to inject light into the TM grating couplers [7]. A polarization maintaining fibre array was used to couple light in/out of the chip [8].

Raw Data

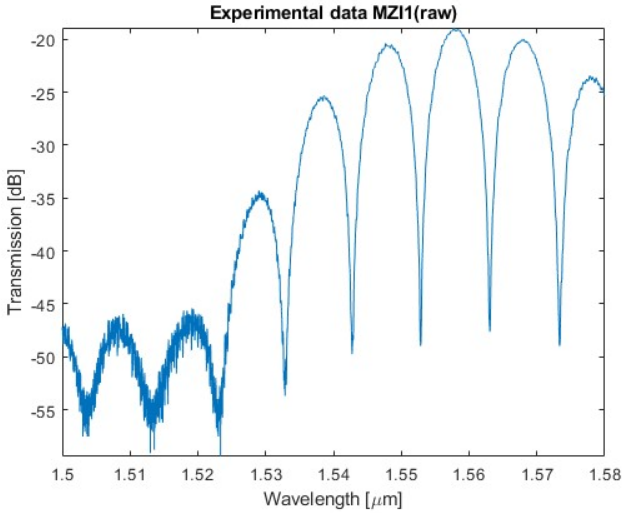

Figure 10: Experimental data of MZI1

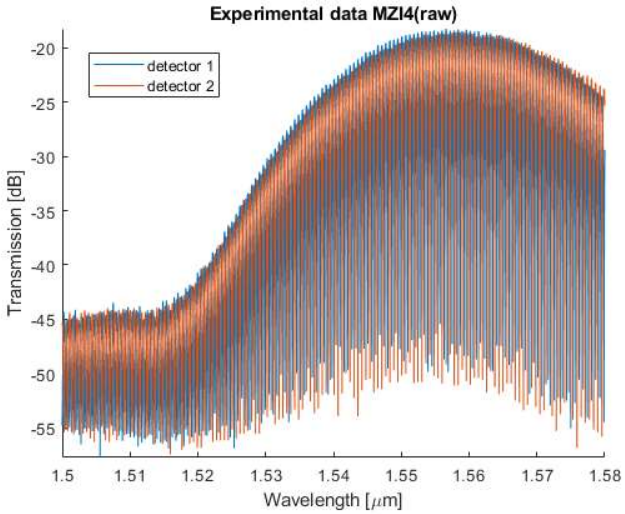

Figure 11: Experimental data of MZI4

VII. Analysis

To perform the data analysis for the MZI's mentioned (MZI 1, 4) in the diagram. A coupling test was performed to determine the proper background reduction and create a baseline from which the data could be fit to determine the group index and free spectral range within the range of approximately 1.53 – 1.57um for the TE polarization devices. One the background subtraction was completed a polynomial fitting with auto correlation was performed to determine the following information. Fitting coefficients, group index, and FSR. The comparison between the two devices which use the mentioned SOI platform have comparable group index for the two different FSR's. The results indicate that for MZI1, across the mentioned wavelength range of interest mentioned:

Fitting coefficients:

$A_1 = 2.4195$
$A_2 = -1.1524$
$A_3 = -0.1491$

Average group index = 4.1982

Average free spectral range = 9.9 nm

For MZI 4 the determined parameters for a path length difference of approximately 971nm are:

Fitting coefficients:

$A_1 = 2.4415$
$A_2 = -1.1242$
$A_3 = -0.0805$

Average group index = 4.1839

Average FSR = 0.585 nm

When curve fitting for the MZI data achieved an R^2 value above .95 indicate good agreement with the experimental data. Comparing the two spectrums, the larger path length difference gives a slightly difference group index for the two devices (0.3412 % difference). Due to the larger path length difference in MZI4, it may be that there is an increased phase sensitivity which gives a slightly more accurate measurement of the group index over the wavelength range of interest.

Comparing between the corner analysis and the expected value. The group indices of the devices fall within the range given from the corner analysis (4.170, 4.249). and the percentage difference from the nominal value for a 500 x 220 nm SOI waveguide group index at 1550nm TE polarization (4.192) are:

MZI1: 0.1479%
MZI4: 0.1932%

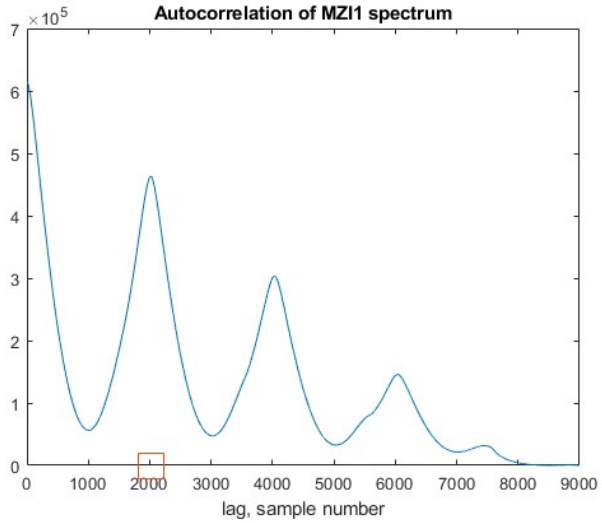

Figure 12: Autocorrelation of MZI1

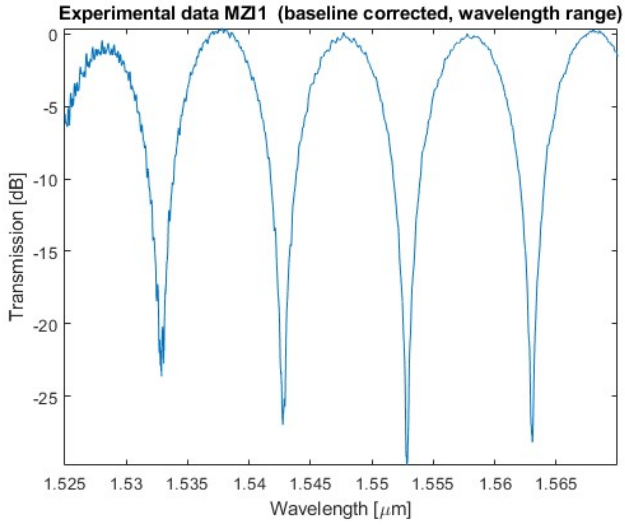

Figure 15: Baseline corrected MZI1 experimental dat

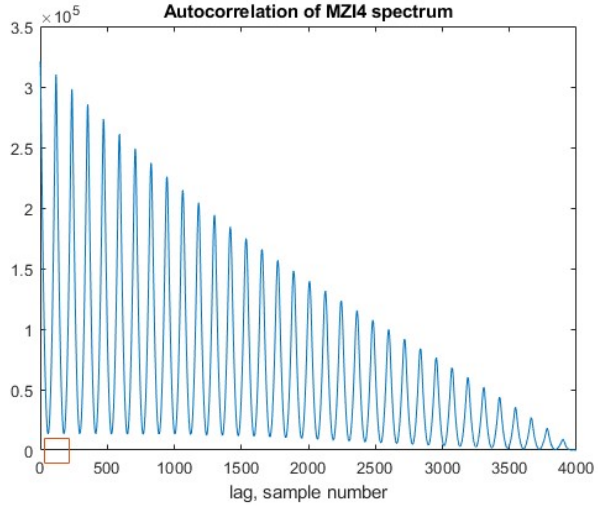

Figure 13: Autocorrelation of MZI4

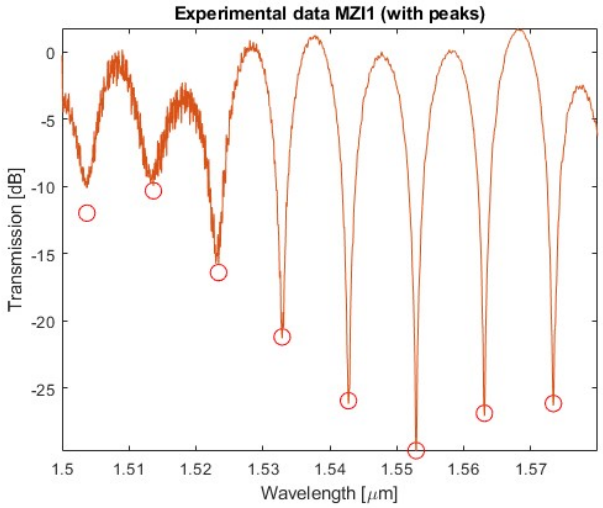

Figure 16: peak finding for MZI1 experimental data

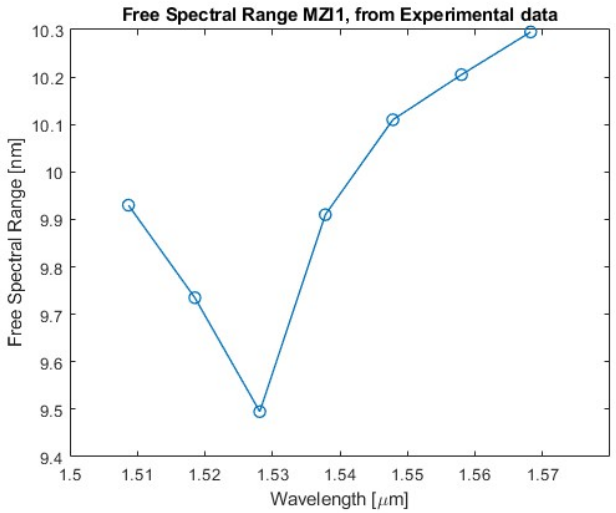

Figure 14: Free spectral range from curve fit of MZI1 data

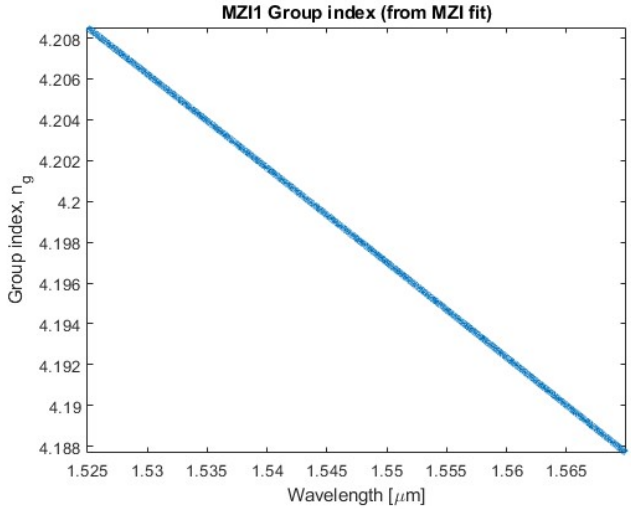

Figure 17: Group index from curve fit of MZI1 data

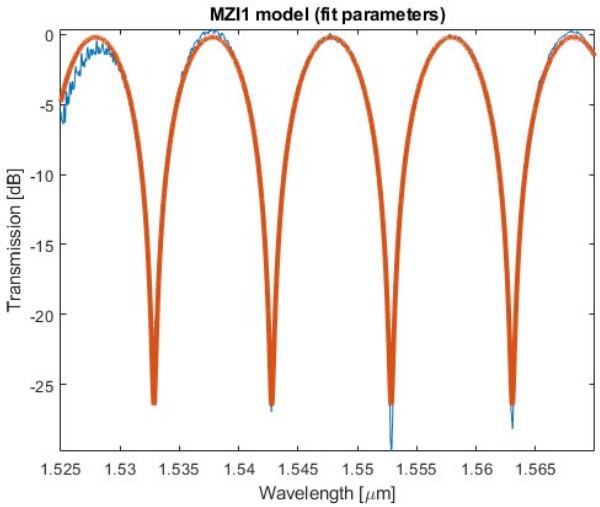

Figure 19: Curve fit of MZI1 data

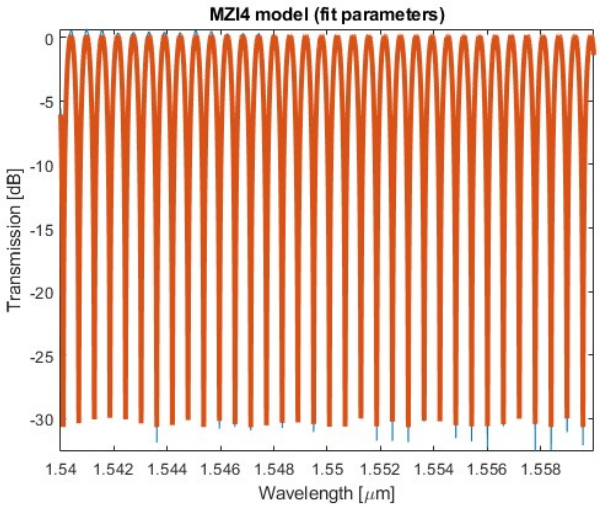

Figure 22: curve fit of MZI4 Experimental data

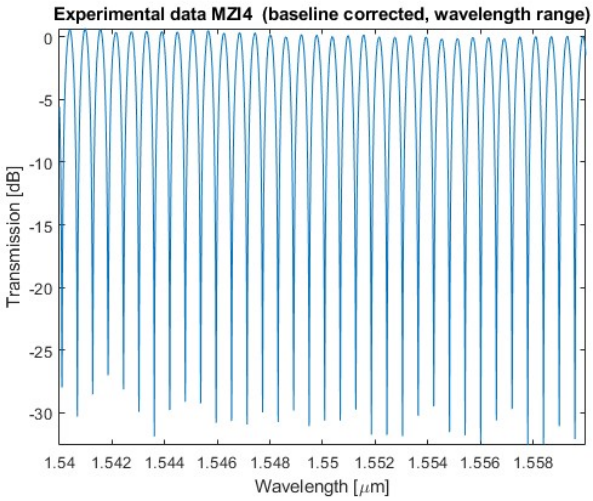

Figure 20: Experimental data of MZI4 baseline corrected

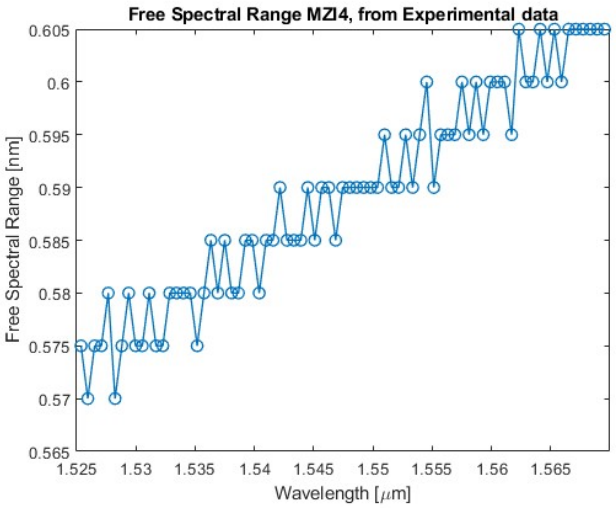

Figure 23: Free spectral range of MZI4 based on experimental data

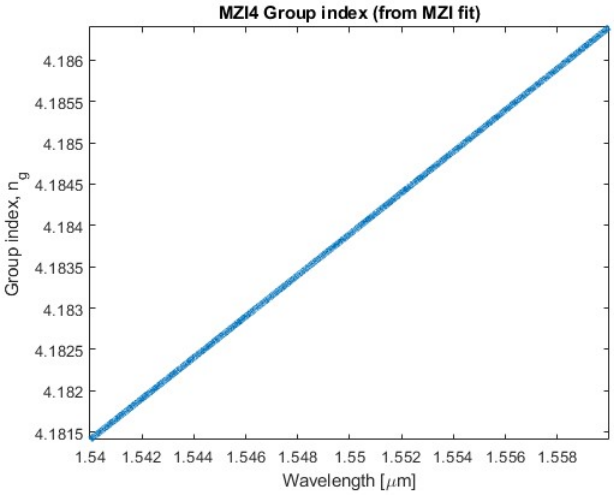

Figure 21: Group index from the curve fit of MZI4 experimental data

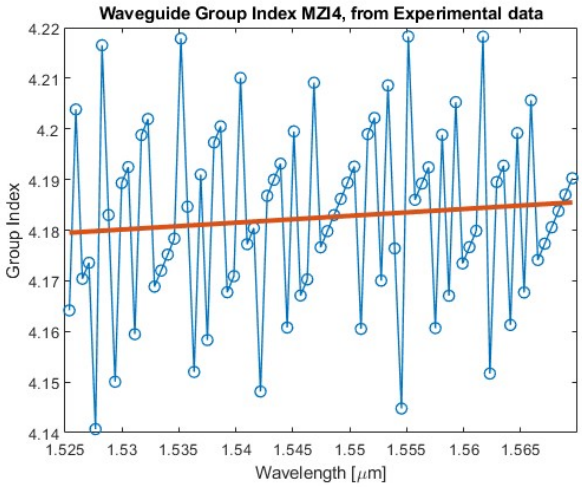

Figure 24: Group index of MZI4 based on experimental data

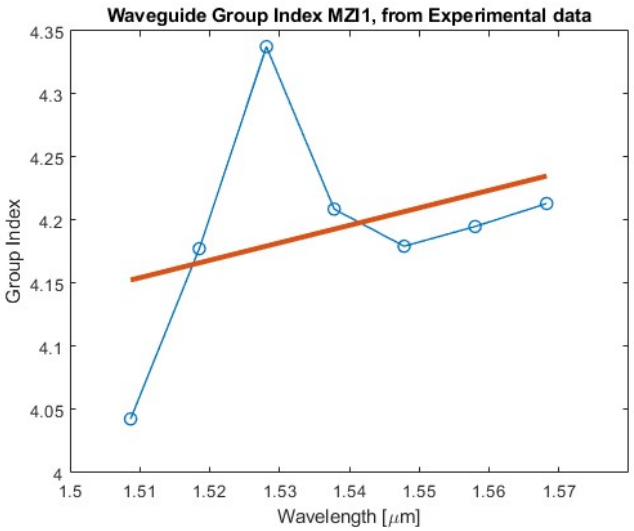

Figure 25: Group index of MZI1 based on experimental data

VIII. Conclusion

From the work discussed in this report, based on the results comparing the experimental results where the group index and free spectral range fall within the accepted range of values for based on the standard deviations from the fabrication that determine the range of values you could have for the group index. The group index of MZI1 and MZI4 are 4.1982 and 4.1839 respectively. With the range of values for the group index, this report draws several conclusions from the techniques used for fabrication and data analysis. The group index of a device can be determined from using the MZI transfer function and free spectral range from the experimental data. The rapid fabrication of silicon photonic structures can be used for creating complex circuits that can be used for signal processing and sensing applications.

Acknowledgments

I acknowledge the edX UBCx Phot1x Silicon Photonics Design, Fabrication and Data Analysis course, which is supported by the Natural Sciences and Engineering Research Council of Canada (NSERC) Silicon Electronic-Photonic Integrated Circuits (SiEPIC) Program.
The devices were fabricated by Richard Bojko at the University of Washington Washington Nanofabrication Facility, part of the National Science Foundation's National Nanotechnology Infrastructure Network (NNIN), and Cameron Horvath at Applied Nanotools, Inc. Enxiao Luan performed the measurements at The University of British Columbia. We acknowledge Lumerical Solutions, Inc., Mathworks, Mentor Graphics, Python, and KLayout for the design software.

References and Footnotes

1. Zhou, Zhiping, Ruixuan Chen, Xinbai Li, and Tiantian Li. "Development Trends in Silicon Photonics for Data Centers." *Optical Fiber Technology*, Special Issue on Data Center Communications, 44 (August 1, 2018): 13–23. https://doi.org/10.1016/j.yofte.2018.03.009.
2. Vilson R. Almeida, Qianfan Xu, Carlos A. Barrios, and Michal Lipson, "Guiding and confining light in void nanostructure," Opt. Lett. 29, 1209-1211 (2004)
3. Bock, Przemek J., Pavel Cheben, Jens H. Schmid, Jean Lapointe, André Delâge, Siegfried Janz, Geof C. Aers, Dan-Xia Xu, Adam Densmore, and Trevor J. Hall. "Subwavelength Grating Periodic Structures in Silicon-on-Insulator: A New Type of Microphotonic Waveguide." *Optics Express* 18, no. 19 (September 13, 2010): 20251. https://doi.org/10.1364/OE.18.020251.
4. E. L. Wooten *et al*., "A review of lithium niobate modulators for fiber-optic communications systems," in *IEEE Journal of Selected Topics in Quantum Electronics*, vol. 6, no. 1, pp. 69-82, Jan.-Feb. 2000, doi: 10.1109/2944.826874. keywords: Lithium niobate;Optical fiber communication;Bandwidth;Electrodes;Optical modulation;Optical fiber devices;Voltage;Optical waveguides;Fabrication;Digital communication},
5. Lukas Chrostowski, Michael Hochberg, chapter 12 in "Silicon Photonics Design: From Devices to Systems", Cambridge University Press, 2015
6. http://siepic.ubc.ca/probestation, using Python code developed by Michael Caverley.
7. Yun Wang, Xu Wang, Jonas Flueckiger, Han Yun, Wei Shi, Richard Bojko, Nicolas A. F. Jaeger, Lukas Chrostowski, "Focusing sub-wavelength grating couplers with low back reflections for rapid prototyping of silicon photonic circuits", Optics Express Vol. 22, Issue 17, pp. 20652-20662 (2014) doi: 10.1364/OE.22.020652
8. www.plcconnections.com, PLC Connections, Columbus OH, USA.
9. http://mapleleafphotonics.com, Maple Leaf Photonics, Seattle WA, USA.